An integrated investigation of the effects of ocean acidification on adult abalone (Haliotis tuberculata)

Solène Avignon, Stéphanie Auzoux-Bordenave, Sophie Martin, Philippe Dubois, Aïcha Badou, Manon Coheleach, Nicolas Richard, Sarah Di Giglio, Loic Malet, Arianna Servili, et al.

An integrated investigation of the effects of ocean acidification on adult abalone (*Haliotis tuberculata*)

S. Avignon *et al.*

The effects of ocean acidification on adult abalone[AQ1]

Solène Avignon[1], Stéphanie Auzoux-Bordenave[1,2*], Sophie Martin[2,3], Philippe Dubois[4], Aïcha Badou[5], Manon Coheleach[6], Nicolas Richard[1], Sarah Di Giglio[4], Loïc Malet[7], Arianna Servili[8], Fanny Gaillard[3], Sylvain Huchette[9], and Sabine Roussel[6][AQ2]

[1]. *UMR "Biologie des Organismes et Ecosystèmes Aquatiques" (BOREA), MNHN/CNRS/SU/IRD, Muséum National d'Histoire Naturelle, Station Marine de Concarneau, Concarneau 29900, France*

[2]. *Sorbonne Université, 4, place Jussieu, Paris 75005, France*

[3]. *UMR 7144 "Adaptation et Diversité en Milieu Marin" (AD2M), CNRS/SU, Station Biologique de Roscoff, Roscoff Cedex 29680, France*

[4]. *Laboratoire de Biologie Marine, Université Libre de Bruxelles, Brussels CP160/15, 1050, Belgium*

[5]. *Direction Générale Déléguée à la Recherche, l'Expertise, la Valorisation et l'Enseignement (DGD REVE), Muséum National d'Histoire Naturelle, Station marine de Concarneau, Concarneau 29900, France*

[6]. *Université de Brest, CNRS, IRD, Ifremer, LEMAR, Plouzané F-29280, France*

[7]. *Service 4Mat, Université Libre de Bruxelles, Brussels CP, 194/3, 1050, Belgium*

[8]. *IFREMER, Université de Brest, CNRS, Plouzané IRD, LEMAR, F-29280, France*

[9]. *Ecloserie France Haliotis, Kerazan, Plouguerneau 29880, France[AQ3]*

Handling editor: Joanna Norkko

*. *Corresponding author: tel: +33 2 98 50 42 88; e-mail: stephanie.auzoux-bordenave@mnhn.fr.*

ABSTRACT

Ocean acidification (OA) and its subsequent changes in seawater carbonate chemistry are threatening the survival of calcifying organisms. Due to their use of calcium carbonate to build their shells, marine molluscs ~~being~~ are particularly vulnerable[AQ4]. This study investigated the effect of CO_2-induced OA on adult European abalone (*Haliotis tuberculata*) using a multi-parameter approach. Biological (survival, growth), physiological (pH_T of haemolymph, phagocytosis, metabolism, gene expression), and structural responses (shell strength, nano-indentation measurements, Scanning electron microscopy imaging of microstructure) were evaluated throughout a 5-month exposure to ambient (8.0) and low (7.7) pH conditions. During the first 2 months, the haemolymph pH was reduced, indicating that abalone do not compensate for the pH decrease of their internal fluid. Overall metabolism and immune status were not affected, suggesting that abalone maintain their vital functions when facing OA. However, after 4 months of exposure, adverse effects on shell growth, calcification, microstructure, and resistance were highlighted, whereas the haemolymph pH was compensated. Significant reduction in shell mechanical properties was revealed at pH 7.7, suggesting that OA altered the biomineral architecture leading to a more fragile shell. It is concluded that under lower pH, abalone metabolism is maintained at a cost to growth and shell integrity. This may impact both abalone ecology and aquaculture. [AQ5]

Keywords: abalone , calcification , gene expression , growth , mechanical properties , ocean acidification , physiology , shell microstructure

Introduction[AQ6]

Over the past 200 years, about one-third of anthropogenic CO_2 emissions have been absorbed by the oceans, resulting in a disruption of carbonate chemistry (Caldeira and Wickett, 2003; Sabine *et al.*, 2004). These changes in the carbo-

nate balance are responsible for a decrease of seawater pH and the lowering of calcium carbonate ($CaCO_3$) saturation state, a process known as ocean acidification (OA; Caldeira and Wickett, 2003; Hoegh-Guldberg *et al.*, 2007; Gattuso *et al.*, 2015). Predictive scenarios suggest a decrease in seawater pH of 0.1–0.4 unit by the end of the 21st century (Orr *et al.*, 2005; IPCC, 2014; Gattuso *et al.*, 2015). OA may affect organisms producing calcium carbonate shells, tests, or skeletons, such as molluscs, corals, and echinoderms, to different extents (Hendriks *et al.*, 2010; Hofmann *et al.*, 2010; Wittmann and Pörtner, 2013; Cyronak *et al.*, 2016). Due to their physiological characteristics and their use of $CaCO_3$ to build their shell, marine molluscs are among the most vulnerable species with regards to OA (Fabry, 2008; Gazeau *et al.*, 2013; Kroeker *et al.*, 2013; Parker *et al.*, 2013). Since proton export from the calcifying space is more energy demanding under OA, metabolic energy demand forcibly rises (Beniash *et al.*, 2010; Parker *et al.*, 2012). Indeed, many species show reduced calcification rates when exposed to acidified seawater (Michaelidis *et al.*, 2005; Gazeau *et al.*, 2007). Furthermore, shell structural and mechanical properties may be affected (Fitzer *et al.*, 2015).[AQ8]

Abalone are ecologically and commercially important molluscs providing essential ecosystem services and food delicacy for humans (Cook, 2016). The European species, *Haliotis* [AQ7]*tuberculata*, is traditionally eaten in Brittany, the Channel Islands, and in some parts of the Mediterranean (Huchette and Clavier, 2004). Whereas production from abalone fisheries worldwide has declined from 20 000 tons in the 1970s to around 6500 tons in recent times due to overfishing and environmental disruptions (Vilchis *et al.*, 2005; Rogers-Bennett, 2007; Travers *et al.*, 2009; Cook, 2016), abalone aquaculture production has significantly increased over the past few years from a negligible quantity in the 1970s to 130 000 tons in 2015 (Cook, 2016). Understanding the effects of environmental stress on abalone biology is an important issue for the management of natural populations as well as for the optimization of fisheries and aquaculture practices (Morash and Alter, 2015).

Haliotis tuberculata is a suitable model for studying the calcification process under OA, since its shell is mainly composed of aragonite (Auzoux-Bordenave *et al.*, 2010), a calcium carbonate polymorph, which is more sensitive to dissolution than calcite (Morse *et al.*, 2007). Captive rearing of abalone is possible for the entire life cycle, making it possible to study the effects of OA under controlled conditions on different development stages (Wessel *et al.*, 2018). Recent study on *H. tuberculata* has shown that larval viability and development were negatively affected at lower pH (7.7 and 7.6) while larval shell showed a reduction in mineralization (Wessel *et al.*, 2018). Adverse effects of OA were also shown in 6-month-old juvenile, with significant decreases in growth and changes in shell microstructure (Auzoux-Bordenave *et al.*, 2019). As suggested by previous studies, the exposure of adult molluscs to OA might also influence shell growth, calcification, and offspring survival (Parker *et al.*, 2013). For example, the intertidal common limpet *Patella vulgata* exposed for a few days to lower pH (7.6) was able to maintain its extracellular acid-base balance, metabolism, and feeding rate, but damage was sustained to the radula of adults, which could compromise feeding and population survival (Marchant *et al.*, 2010). In adult oyster *Crassostrea virginica*, physiology and rates of shell deposition appeared to be negatively affected by OA, with an increase in carbonic anhydrase (CA) expression in tissues of animals exposed to reduced pH water (Beniash *et al.*, 2010). So far, no studies have been conducted on the adult stage of European abalone *H. tuberculata*.

The goal of the present study was to investigate the effects of a 5-month exposure to CO_2-induced OA on adult abalone using a multi-parameter approach. Four-year abalone *H. tuberculata* were exposed during reproductive conditioning to ambient seawater pH (8.0) and to a lower pH value (7.7) corresponding to the projected decrease of −0.3 pH units under RCP 8.5 climate change scenario (IPCC, 2014; Gattuso *et al.*, 2015). Several biological parameters involved in growth, physiology, and metabolism were measured on individuals exposed to either current or near-future pH conditions. Shell microstructure and mechanical properties were also analysed to assess whether reduced pH has an influence on shell integrity.

Material and methods

Abalone collection and acclimation

Adult *H. tuberculata* (n = 260, 48.5 ± 4.2 mm shell length, 16.2 ± 4.4 g shell weight), from a spawning performed during summer 2013, were selected at random from an offshore sea-cage structure containing 600 individuals per cage, at the France Haliotis abalone farm in January 2017 (48°36′50N, 4°36′3W; Plouguerneau, Brittany, France).

Fresh algae collected on the shore were provided *ad libitum* to each sea-cage once a month. The algae were composed of mixture of *Palmaria palmata*, *Laminaria digitata*, and *Saccharina latissima*, depending on the season (S Huchette, pers. comm.). Abalone were brought to the France Haliotis land-based facilities ensuring minimum stress during transport and minimum handling. After measuring size and weight, each abalone was randomly distributed in ten 45 l aquaria (l × w × h, 50 × 30 × 35 cm) equipped with baked clay hiding places (n = 26 abalone per aquarium). An aeration system was placed in each aquarium. Animals were conditioned for 3 weeks in the laboratory under ambient pCO_2/pH conditions, in aquaria supplied with a minimum of 15 l h^{-1} of 3 µm filtered seawater at ambient temperature. The seawater was pumped from close to the farm. During the experimentation, abalone were fed once a week *ad libitum* with the macroalgae *P. palmata*. The aquaria were cleaned twice a week using a siphoning hose and water filters were changed every day.

Experimental set-up

Each experimental aquarium was randomly assigned to one of two pH treatments (Figure 1): a control condition corresponding to the local seawater pH (8.0, pCO_2 around 460 µatm) and a lower pH value (7.7, pCO_2 around 1000 µatm) corresponding to the projected decrease of −0.3 pH units under climate change scenario RCP 8.5 (IPCC, 2014; Gattuso *et al.*, 2015). Five replicate aquaria were used per pH condition. Photoperiod was adjusted following the seasonal cycle with a dimmer (Gold Star, Besser Elektronik, Italy). The experiment was carried out for 5 months between February and July 2017. At the beginning of the experiment, pH was gradually decreased over 6 d by 0.05 pH units/day until pH 7.7 was reached.

Figure 1. Experimental design. Seawater was continuously pumped into the ten 60-l header tanks. The pH was adjusted in CO_2 enriched header tanks by bubbling CO_2 through electro-valves and controlled by the IKS system (grey tanks for pH 8.0, white tanks for pH 7.7). From the header tanks, the CO_2-enriched water and the control water flowed down to 45 l experimental aquaria. Each aquarium contained 26 adult abalone (i.e. there were a total of 130 abalone per pH treatment).

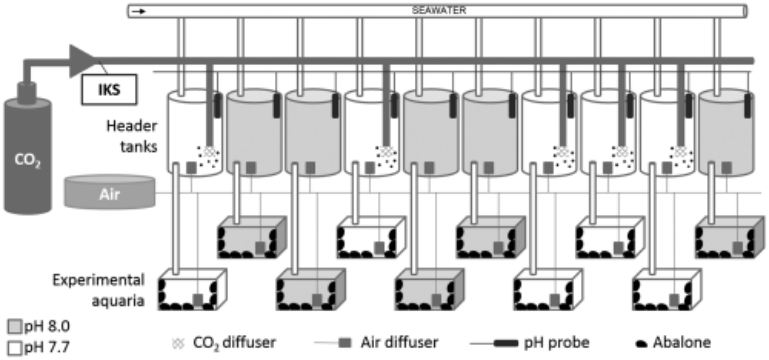

pH and carbonate system monitoring

Inside a storage tank (9000 l), seawater was temperature-controlled with a heat pump and used to continuously fill the ten header tanks. Each header tank supplied one experimental tank at a rate of 15 l h^{-1}. In the five CO_2-enriched header tanks, pCO_2 was adjusted by bubbling CO_2 (Air Liquide, France) through electro-valves controlled by a pH-stat system (IKS Aquastar, Germany). pH values of the pH-stat system were adjusted from measurements of the electromotive force using a pH meter (Metrohm 826 pH mobile, Metrohm, Switzerland) with a glass electrode (Primatrode). The electromotive force was converted to pH units on the total scale (pH_T) after calibration with Tris/HCl and 2-aminopyridine/HCl buffers (Dickson, 2010).

Seawater parameters were recorded every 3 d throughout the 5-month experiment. Temperature was regulated at 2°C above the monthly average temperature observed in local environment (10.5°C in January to 16.5°C in June) in order to stimulate gonad development. pH_T was measured every 3 d in each experimental aquaria using a pH meter as described above. Temperature and salinity were measured daily with a conductimeter (WTW 3110, Germany). Total alkalinity (A_T) of seawater was measured monthly on 100-ml samples taken from incoming water and from each experimental tank. Seawater samples were filtered through 0.7-µm Whatman GF/F membranes, immediately poisoned

with mercuric chloride and stored in a cool dark place pending analyses. A_T was determined potentiometrically using an automatic titrator (Titroline alpha, Schott SI Analytics, Germany) calibrated with the National Bureau of Standards scale. A_T was calculated using a Gran function applied to pH values ranging from 3.5 to 3.0 as described by Dickson *et al.* (2007) and corrected by comparison with standard reference material provided by A. G. Dickson (CRM Batch 111). Temperature, salinity, pH_T, and A_T were used to calculate the carbonate system parameters: pCO_2, dissolved inorganic carbon (DIC), HCO_3^-, CO_3^{2-} concentrations, and saturation state of aragonite ($\Omega_{aragonite}$) and calcite ($\Omega_{calcite}$). Calculations were performed using CO_2SYS software (Pierrot *et al.*, 2006) set with constants of Mehrbach *et al.* (1973) refitted by Dickson and Millero (1987).

Abalone sampling

The effects of OA were examined at different sampling times. Firstly, the short-term exposure response was analysed after 1 week (W1, 6 d) of pH exposure. Afterwards, samplings were done regularly every month: at 2 months (M2, 60 d), 3 months (M3, 90 d), 4 months (M4, 125 d), and 5 months (M5, 157 d).

At each sampling time, abalone were randomly collected for biometric measurements. Physiological measurements were performed on haemolymph sampled for some individuals (see below), while metabolic parameters were measured on live animals. Mantle tissue was dissected and rapidly frozen in liquid nitrogen for gene expression analyses. The shells were rinsed with distilled water, dried, and stored at room temperature until analysis. Abalone were only used once in the experiment and were not returned to the aquaria after measurement. Some individuals were used for two types of measures (e.g. physiological and biometric measures).

Survival

Abalone survival was assessed every day along the experiment and any dead individuals were removed from the tanks immediately. Survival (%) was calculated as the proportion of living individuals after the 5-month treatment vs. total number of abalone per aquarium at the beginning of the experiment, minus the individuals sacrificed for analysis.

Biometric measurements

Biometric measurements were performed at W1, M2, M3, M4, and M5 of exposure. At each sampling time, length (mm) was measured using a manual calliper to the nearest 0.5 mm to obtain the growth in length in millimetre per day on two to five abalone per aquarium (n = 13–39 abalone per pH treatment). Except at M5, individuals were weighed using an analytical balance to the nearest 0.01 mg to obtain specific growth rate using natural log mass values (% gain/day). Haemolymph was sampled in <1 min from the pedal sinus, using a refrigerated 2-ml syringe and 25 G × ½ needles. It was transferred to a vial on ice and processed immediately after collection to avoid haemocyte aggregation. After a section of the head, tissues and organs were dissected. The weight of the foot muscle, gonad, shell, and haemolymph was recorded to the nearest 0.01 mg.

Physiological measurements

The pH_T of the haemolymph was measured immediately on two abalone per aquarium (n = 10 per pH treatment), at W1, M2, and M4. The electromotive force of the haemolymph was measured with a glass electrode put into the vial. Temperature was also measured to obtain pH_T according to the procedure described above for seawater pH_T determination. Phagocytosis efficiency was measured according to a protocol adapted from Travers *et al.* (2008), using two replicates of 25-µl haemolymph. In brief, 25 µl of haemolymph was deposited into a 24-well plate containing 100 µl of sterile seawater. Haemocytes were allowed to adhere for 15 min at 18°C. Fluorescent beads (gluoresbrite YG Microspheres 2.00 mm, Plysciences, 1:100 in distilled water) were added. After 2 h at 18°C, supernatants were removed and 100 µl of trypsin (2.5 mg ml^{-1} in AASH) was added to detach the adherent cells. Plates were shaken for 10 min. Then, 100 µl of 6% formalin was used to stop the reaction. Analyses were performed on a FACS-Calibur flow cytometer (Becton Dickinson, France) equipped with a 488-nm laser. Data were analysed using the WinMDI program. Phagocytosis efficiency was defined as the percentage of haemocytes that had engulfed three or more beads.

Gene expression analysis

The expression profile of selected genes was analysed in the mantles of two to four individual abalone per aquarium (n = 17 for pH 8.0 and n = 14 for pH 7.7) after 4 months of pH treatment (M4). Genes were chosen with respect to their putative functions in shell growth and calcification responses and their abundance in the mantle transcriptomes (Shen *et al.*, 1997; Le Roy *et al.*, 2012). One gene involved in shell biomineralization, Lustrin A, two CAs involved in bicarbonate ions formation (CA 1 and CA 2), and genes for two stress proteins (heat shock proteins), HSP71 and HSP84, were targeted by using specific primers (Table 1). 18S and EF1 were used as reference genes.

Table 1. Specific primers used for gene expression analysis in *Haliotis tuberculata*: GenBank accession numbers, primer sequences, and references.

Gene	Accession numbers	Sequence 5′–3′	References
Lustrin A	HM852427.2	F-ATCTGTCCGGCAGTTCCTAC	Gaume *et al.* (2014)
		R-CTGGGGCACTGTAAGTTGGT	
CA1	HQ845770.1	F-ATGGCAGCTGATAAAGCAAC	Designed for the study
		R-AGGGAAATGAGTGTGCATGT	
CA2	HQ845771.1	F-CGCCGACTTTATCTGAGAGC	Le Roy *et al.* (2012)
		R-GTCTCCCACGAAGTGGTTGT	
18S	AF120511.1	F-GGTTCCAGGGGAAGTATGGT	Gaume *et al.* (2014)
		R-AGGTGAGTTTTCCCGTGTTG	
EF1	FN566842.1	F-ATTGGCCACGTAGATTCTGG	Gaume *et al.* (2014)
		R-GCTCAGCCTTCAGTTTGTCC	
HSP 71	AM283516.1	F-CGGTGAGCGCAATGTTC	Farcy *et al.* (2007)
		R-CCAAGTGGGTGTCTCCA	
HSP 84	AM283515.1	F-CCAGGAAGAATATGCCGAGT	Farcy *et al.* (2007)
		R-CACGGAACTCCAACTGACC	

Frozen mantle samples were pulverized under liquid nitrogen using a Retsch MM400 mixer mill. Total RNA was extracted from the resulting powder using Extract-all reagent (Eurobio, Courtaboeuf, Essonne, France) followed by chloroform phase separation and isopropanol precipitation. The co-extracted DNA was then digested with an RTS DNase Kit (MoBio). The quantity, purity, and quality of RNA were assessed using an ND-1000 NanoDrop® spectrophotometer (Thermo Scientific Inc., Waltham, MA, USA) and by electrophoresis using an Agilent Bioanalyser 2100 (Agilent Technologies Inc., Santa Clara, CA, USA). cDNA synthesis was performed using an iScript™ cDNA Synthesis kit (Bio-Rad Laboratories Inc., Hercules, CA, USA). Reverse transcription-quantitative PCR (RT-qPCR) was conducted in a C1000 Touch Thermal Cycler (Bio-Rad Laboratories Inc., Hercules, CA, USA) using specific primers (see Table 1) and SsoAdvanced Universal SYBR Green Supermix (Bio-Rad Laboratories Inc., Hercules, CA, USA) as described by Cadiz *et al.* (2017). Gene expression was quantified using the iCycler MyiQ™ Single-Color Real-Time PCR Detection System (Bio-Rad Laboratories Inc.). The relative quantity of messenger was normalized with the ΔCt method using the same CFX Manager software (Bio-Rad Laboratories Inc.).

Metabolic rates

Calcification, respiration, and excretion rates were determined using two to three individual abalone per aquarium at W1, M2, and M3 (n = 9–15 abalone per pH treatment). Individuals were incubated individually in a 598-ml acrylic chamber (Engineering & Design Plastics Ltd, Cambridge, UK) filled with seawater from their respective aquaria. Incubations lasted 1 h. Blank incubations were also carried out with only seawater from the aquarium to adjust respiration and excretion rates.

Oxygen concentrations were measured at the beginning and the end of the incubation period with a non-invasive fibre-optics system (FIBOX 3, PreSens, Regensburg, Germany). Reactive oxygen spots attached to the inner wall of

the chambers were calibrated with 0% and 100% oxygen buffers. Seawater was sampled for ammonium (NH_4^+) concentration with 100-ml syringes at the beginning of the incubation, directly in the aquaria just after the chambers were closed, and at the end of the incubation, in the incubation chamber itself. Samples were fixed with reagent solutions and stored in the dark. NH_4^+ concentrations were determined according to the Solorzano method (Solorzano, 1969) based on spectrophotometry at a wavelength of 630 nm (spectrophotometer UV-1201V, Shimadzu Corp, Kyoto, Japan). A_T (in µEq/l) values were obtained in the same way as described above in the section *pH and carbonate system monitoring*. Respiration [in µmol O_2/g WW/h; Equation (1)] and excretion [in µmol NH_4^+/g WW/h; Equation (2)] rates were directly calculated from oxygen and ammonium concentrations, respectively. Net calcification [in µmol $CaCO_3$/g WW/h; Equation (3)] rate was estimated using the alkalinity anomaly technique (Smith and Key, 1975) based on decrease in A_T by two equivalents for each mole of $CaCO_3$ precipitated (Wolf-Gladrow *et al.*, 2007). As ammonium production increases alkalinity in a mole-per-mole ratio (Wolf-Gladrow *et al.*, 2007), the alkalinity variation was corrected by the ammonium flux to calculate $CaCO_3$ fluxes.

$$R = \frac{\Delta\, O_2 \times V}{\Delta\, t \times WW} \quad (1)$$

$$E = \frac{\Delta\, NH_4^+ \text{ x V}}{\Delta\, t \times WW} \quad (2)$$

$$G = \frac{-(\,\Delta\, A_T - \,\Delta\, NH_4) \text{ x } V}{2x\,\Delta\, txWW}\,, (3)$$

where $\Delta\, O_2$ (in µmol O_2/L), $\Delta\, NH_4^+$ (in µmol NH_4^+/L), and $\Delta\, A_T$ (in µEq/L) are the differences between initial and final O_2 concentrations, NH_4^+ concentrations, and total alkalinity, respectively; V (in l) is the volume of the chamber minus *H. tuberculata* volume; $\Delta\, t$ (in h) is the incubation time; and WW (in g) is the soft tissue wet weight of the incubated *H. tuberculata*.

Shell analysis

Two to nine shells per aquarium (n = 10–39 abalone per pH treatment) were examined at M2, M3, M4, and M5. The thickness (mm) of the shell newly formed during the experiment was determined as the average of three measurements closest to the edge of the shell, along the growth axis (Supplementary Figure S1a) to the nearest 0.001 mm using a Mitutoyo® digital calliper. Abalone shells were imaged with the NIS elements software (Nikon, Japan) under a binocular microscope (Leica, Germany). For the evaluation of periostracum morphology, the shell surface was imaged and analysed for differences in grey scale. Image-J software was used to calculate an average grey value from zero (black) to 255 (white). The average of grey levels was calculated from a 4 mm^2 area closest to the shell edge, along the growth axis (Supplementary Figure S1a).

To analyse shell surface microstructure, four abalone shells per pH treatment were randomly chosen for further investigation of the inner and outer surfaces by scanning electron microscopy (SEM; Supplementary Figure S1b). The shell was cut in order to obtain a shell fragment formed during the experiment. Samples were gold-coated (Cressington 108, Auto Sputter coater) and observed at 5–15 kV with an SEM (SEM FEI Sigma 300, MNHN, Concarneau, France).

To determine the influence of seawater acidification on shell microstructure and thickness, cross-sections were obtained using a razor blade along the longitudinal growth axis of the shell (Supplementary Figure S1c). Samples were embedded in epoxy resin, gold-coated, and observed as described above. Three transects were determined on SEM images of the cross-sections: in the old part, intermediate part, and newly formed shell area. Within each transect, images were generated from the outer periostracum to the inner nacreous layer, passing through the spherulitic layer.

At higher magnification, the aragonite tablet thickness (average of 25 measurement points) was determined from both old and recent nacre on SEM images with Image-J (n = 3 shells per pH treatment). The thickness of the periostracum, the spherulitic, and nacreous layers was determined from the cross-section images using Image-J software (n = 5 abalone shells per treatment, 20 measurement points per layer).

Biomechanical tests

Shell strength (resistance) was measured individually (n = 10 shells per pH treatment) at M4 using a simple compression method. The comparison of shell fracture force was performed on shells with a similar size and shape. Abalone shells were placed always in a same way on a homemade steel block with their opening downwards (i.e. in the natural position they would have on a rocky substrate) and the mechanical test was carried out using a second homemade steel block (7 × 5 × 2 cm) fixed on the load frame of a force stand (Instron 5543) through a threaded shaft. Care was taken that the two blocks were strictly parallel. The second block was lowered onto the shell at a speed of 0.3 mm min^{-1} (simple compression test) until fracture. Displacement (mm) and compression force (N) were recorded continuously at a frequency of 10 Hz.

Nano-indentation measurements were performed to characterize the properties of the material, i.e. the shell nano-hardness and Young's modulus of elasticity. The other fragment obtained from the earlier cross-section (for SEM) was polished using sandpapers of decreasing grain size (from 52 to 5 µm) to obtain a homogeneous surface (n = 4 shells per pH treatment). Nano-indentation measurements were performed using a Triboindenter (Hysitron, USA) with a Berkovich tip and a charge of 1500 µN. Nano-hardness (GPa) and Young's modulus of elasticity (GPa) were calculated automatically from the unloading curve of the indentation test. For each individual abalone, three profiles spaced by 5–8 mm were made in the newly formed, intermediate, and older zones. Each profile consisted of three continuous transects through the two layers (external layer and nacre) spaced by 5 µm apart. Each transect consisted of 61 indents (26–31 indents per layer). Because values recorded in the three transects of each zone did not differ significantly, the results from the three transects were pooled.

Statistical analysis

All statistical analyses were performed with R software (R Core Team, 2015). Differences between the two pH treatments, except for the biomechanical tests, were tested using linear mixed models with the lmerTest package (Kuznetsova *et al.*, 2017) based on the methods described by Winter (2013). This model used the pH as a fixed factor and aquarium as a random factor nested within the factor pH. Since biometric measurements were performed on abalone that had already been used for metabolism and physiological assessments (at W1, M2, and M4), a test effect was included in the mixed model for those variables. Statistical analysis was performed on the data separately for each time point. For shell, haemolymph, muscle, and gonad weights, total weight was integrated as a covariate in the mixed model. A Student's t-test was used to compare the mortality and thickness of nacreous platelets between the two pH treatments. To be sure to only evaluate the effect of OA on shell resistance, the relationship between the shell fracture force and biometric parameters (shell length, weight, area, and thickness) was tested using a linear regression.

The normality of the residuals and homogeneity of the variance were verified (Shapiro–Wilk and Bartlett tests). When assumptions of homogeneity of variance and normal distribution of residuals were not confirmed, the data were log or inverse transformed before analysis. If these assumptions were not validated, a Welch test was performed using the aquarium value as individual in the statistical test. Differences were considered significant at $p < 0.05$. Data are presented as means of squares ± standard error unless otherwise indicated. All results in graphs are presented as boxplots showing the median, the second and third quartiles (boxes), the 95% confidence interval (whiskers) and outside of the 95 percentile range values (o).

Mechanical data were analysed using the cumulative probability function:

$$P_{fi} = 1 - \exp\left(-\left(\frac{\sigma_i}{\sigma_0}\right)^m\right),$$

which is also known as the Weibull three-parameter strength distribution. p_f is the probability of failure that increases with the stress variable, σ. The characteristic stress σ_0 is an experimentally obtained parameter that corresponds to a proportion of fractured samples of (1 − 1/e) = 63% (cumulative failure probability). In this study, we replaced the stress variable by nano-hardness (H_0) and Young's modulus of elasticity (E_0) and used the linearized curve of Weibull statistical analysis to calculate the 95% confidence intervals of E_0 and H_0 (corresponding to the 63 percentiles for Young's modulus of elasticity and nano-hardness, respectively) with the modified least square regression of Bütikofer *et al.* (2015). This allowed statistical comparisons, based on 95% confidence intervals, for each layer, zone, and pH.

Results

Seawater parameters

Mean seawater carbonate chemistry parameters are presented in Table 2. Seawater temperature followed natural variations and ranged from 12.6°C ± 0.7°C at the start of the experimental period (in February) to 16.5°C ± 0.5°C at the end (in June/July). Salinity was 34.6 ± 0.6 in all experimental aquaria and remained stable over the experiment. Total alkalinity (A_T) measured in the experimental tanks was 2355 ± 9 µEq. kg^{-1} and remained stable over the experiment and between all aquaria. The pH_T in aquaria was maintained close to nominal value along the experiment, with 8.01 ± 0.05 (pCO_2 439 ± 57 µatm) in control aquaria and 7.71 ± 0.06 (pCO_2 951 ± 138 µatm) in lower pH aquaria. $\Omega_{aragonite}$ was 2.30 ± 0.31 and 1.25 ± 0.19 and $\Omega_{calcite}$ was 3.59 ± 0.46 and 1.95 ± 0.28 in pH 8.0 and pH 7.7 conditions, respectively.

Table 2. Seawater temperature, salinity, and parameters of the carbonate system in each pH treatment (i.e. pH 8.0 and pH 7.7, n = 5 per treatment).

Carbonate system parameter	pH 8.0	pH 7.7
Nominal pH	8.0	7.7
pH_T	8.01 ± 0.05	7.71 ± 0.06
Temperature (°C)	14.4 ± 1.4	14.4 ± 1.5
Salinity	34.6 ± 0.6	34.6 ± 0.6
pCO_2 (µatm)	439 ± 57	951 ± 138
DIC (µmol kg^{-1})	2150 ± 28	2277 ± 25
HCO_3^- (µmol kg^{-1})	1984 ± 48	2154 ± 30
CO_3^{2-} (µmol kg^{-1})	151 ± 20	82 ± 12
$\Omega_{aragonite}$	2.30 ± 0.31	1.25 ± 0.19
$\Omega_{calcite}$	3.59 ± 0.46	1.95 ± 0.28

Seawater pH on the total scale (pH_T), temperature, salinity, and total alkalinity (mean 2355 ± 9 µEq. kg^{-1}) was used to calculate CO_2 partial pressure (pCO_2; µatm), dissolved inorganic carbon (DIC; µmol kg^{-1}), HCO_3^- (µmol kg^{-1}), CO_3^{2-} (µmol kg^{-1}), aragonite saturation state (Ω_{ar}), and calcite saturation state (Ω_{calc}) by using the CO_2SYS program. Values are mean ± *SD*.

Survival, biometry, and growth

Abalone survival after 5 months of exposure to lowered pH was very high with no difference between individuals exposed to pH 8.0 and pH 7.7 (96.9% and 95.4%, respectively, Table 3).

Table 3. Summary of mixed model results used to test the effect of pH on studied parameters in adult abalone (pH: fixed factor, tank: random factor) after 1 week (W1), 2 (M2), 3 (M3), 4 (M4), and 5 (M5) months of exposure.

Parameter	W1	M2	M3	M4	M5
Survival	–	–	–	–	$t_{258} = -0.64$, $p = 0.521$ [2]
Shell growth in length	–	$F_{1, 36} = 2.11$, $p = 0.155$	$F_{1, 26} = 0.20$, $p = 0.655$	$F_{1, 34} = 0.03$, $p = 0.866$	**$F_{1, 8} = 7.25$, $p = 0.027$**
Specific growth rate	–	**$F_{1, 24} = 4.77$, $p = 0.039$**	$F_{1, 24} = 0.39$, $p = 0.539$	$F_{1, 7} = 0.02$, $p = 0.887$	–
Haemolymph weight	$F_{1,9} = 4.01$, $p = 0.078$	$F_{1,10} = 1.39$, $p = 0.267$	$F_{1,24} = 3.98$, $p = 0.058$	$F_{1,7} = 0.41$, $p = 0.544$	–
Muscle weight	$F_{1,14} = 0.02$, $p = 0.905$	$F_{1,34} = 1.12$, $p = 0.298$	$F_{1,8} = 3.64$, $p = 0.091$	$F_{1,43} = 0.54$, $p = 0.467$	–
Gonad weight	$F_{1,15} = 0.26$, $p = 0.619$	$F_{1,33} = 0.07$, $p = 0.793$	$F_{1,24} = 2.19$, $p = 0.152$	**$F_{1,8} = 5.84$, $p = 0.043$**	–
Haemolymph pH_T	**$F_{1,8} = 11.77$, $p = 0.009$**	**$F_{1,8} = 21.67$, $p = 0.002$**	–	$F_{1,8} = 4.63$, $p = 0.064$	–
Phagocytosis efficiency	$F_{1,8} = 0.07$, $p = 0.802$	$F_{1,8} = 0.89$, $p = 0.373$	–	$F_{1,5} = 0.57$, $p = 0.484$ [1]	–
Respiration rate	$F_{1,8} = 0.52$, $p = 0.493$	$F_{1,8} = 0.05$, $p = 0.827$	$F_{1,25} = 0.99$, $p = 0.328$	–	–
Excretion rate	$F_{1,6} = 0.34$, $p = 0.582$ [1]	$F_{1,4} = 1.75$, $p = 0.253$ [1]	$F_{1,9} = 0.04$, $p = 0.849$	–	–
Gene expression: Lustrin A	–	–	–	$F_{1,6} = 0.66$, $p = 0.446$	–
Gene expression: HSP71	–	–	–	$F_{1,6} = 0.72$, $p = 0.429$ [1]	–
Gene expression: HSP84	–	–	–	$F_{1,7} = 0.10$, $p = 0.757$	–
Gene expression: CA1	–	–	–	$F_{1,26} = 0.06$, $p = 0.802$	–
Gene expression: CA2	–	–	–	$F_{1,5} = 2.49$, $p = 0.178$ [1]	–
Shell coloration	$F_{1,8} = 3.28$, $p = 0.107$	**$F_{1,8} = 49.83$, $p<0.001$**	**$F_{1,8} = 52.51$, $p<0.001$**	**$F_{1,8} = 51.58$, $p<0.001$**	**$F_{1,9} = 172.10$, $p<0.001$**
Net calcification rate	**$F_{1,27} = 7.83$, $p = 0.009$**	$F_{1,8} = 0.33$, $p = 0.582$	**$F_{1,25} = 12.78$, $p = 0.001$**	–	–
Shell weight	$F_{1,43} = 0.01$, $p = 0.913$	$F_{1,9} = 2.49$, $p = 0.149$	$F_{1,24} = 3.59$, $p = 0.070$	$F_{1,30} = 0.46$, $p = 0.501$	$F_{1,8} = 4.81$, $p = 0.059$
Shell thickness	$F_{1,8} = 1.49$, $p = 0.257$	$F_{1,36} = 0.27$, $p = 0.608$	$F_{1,8} = 3.30$, $p = 0.106$	$F_{1,35} = 0.04$, $p = 0.844$	$F_{1,7} = 3.54$, $p = 0.099$
Periostracum thickness	–	–	–	**$F_{1,5} = 28.84$, $p = 0.002$**	–

Parameter	W1	M2	M3	M4	M5
Spherulitic layer thickness	–	–	–	$F_{1,8} = 6.10^{-4}$, $p = 0.982$	–
Nacre layer thickness	–	–	–	$F_{1,8} = 0.08$, $p = 0.785$	–
Platelet thickness	–	–	–	$t_4 = -0.64$, $p = 0.556$ (2)	–
Shell fracture force	–	–	–	**$F_{1,18} = 6.53$, $p = 0.020$**	–

A Welch's heteroscedastic F (1) or a Student's t-test(2) was used when necessary. Significant results are shown in bold ($p < 0.05$).

At M5, abalone exposed to pH 8.0 grew at a rate of 0.039 ± 0.003 mm day^{-1} while the growth rate of those exposed to pH 7.7 was significantly lower, at 0.027 ± 0.003 mm day^{-1} (Figure 2a, Table 3). No differences in growth rate were observed at earlier sampling times (Table 3).

Figure 2. (a) Shell growth in length (n = 13–39 per pH treatment) and (b) specific growth rate (n = 13–26 per pH treatment) of adult abalone exposed to two pH levels (8.0 and 7.7), after 2 (M2), 3 (M3), 4 (M4), and 5 (M5) months of exposure. Significant difference is indicated by * ($p < 0.05$, mixed model).

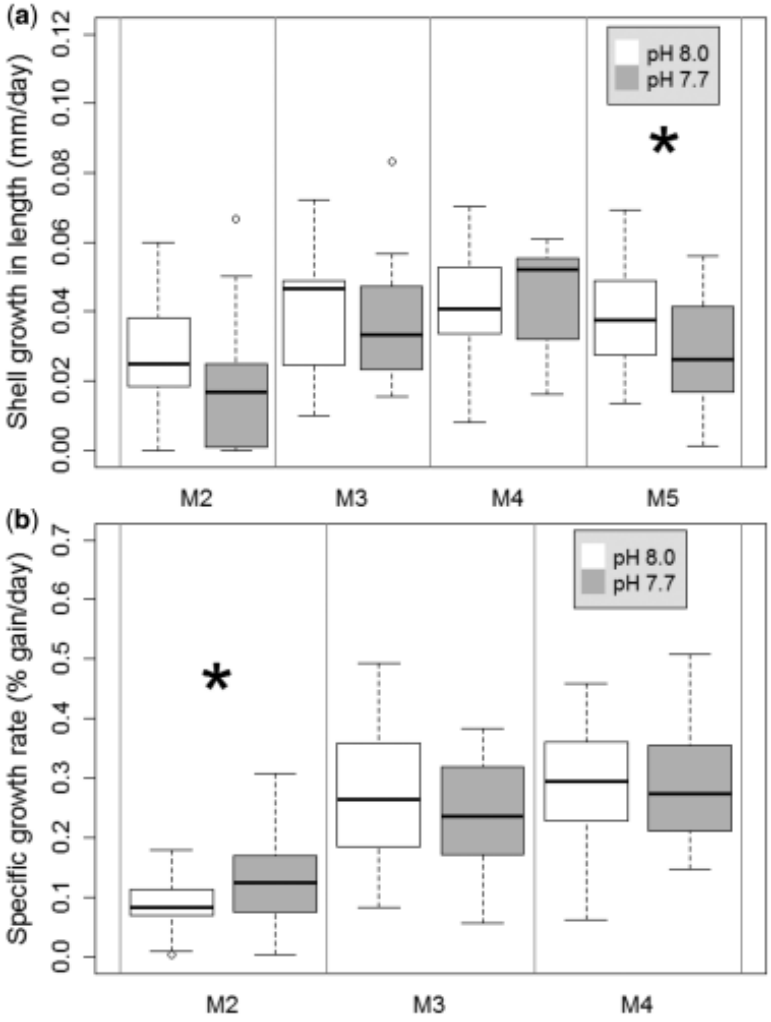

After 2 months of pH exposure at the two levels, specific growth rate was lower for abalone exposed to pH 8.0 compared with abalone exposed to pH 7.7 (Table 3, Figure 2b). No significant differences in specific growth rate were observed at M3 and M4 between the control and low pH groups.

No significant difference was observed for the haemolymph or muscle weights (Table 3). However, at M4, the gonad weight was significantly lower for individuals exposed to pH 7.7. (1.38 ± 0.14 g, Table 3) compared with those exposed to pH 8.0 (1.75 ± 0.13 g).

Physiology and metabolism

The pH_T of haemolymph in abalone exposed to pH 7.7 was significantly lower than those exposed to pH 8.0 at W1 and M2 and a non-significant decrease was observed at M4 (Table 3, Figure 3).

Figure 3. pHT of adult abalone haemolymph exposed to two pH levels (8.0 and 7.7), after 1 week (W1), and 2 (M2) and 4 (M4) months of exposure (n = 7–10 per pH treatment). Significant differences are indicated by * ($p < 0.05$, mixed model).

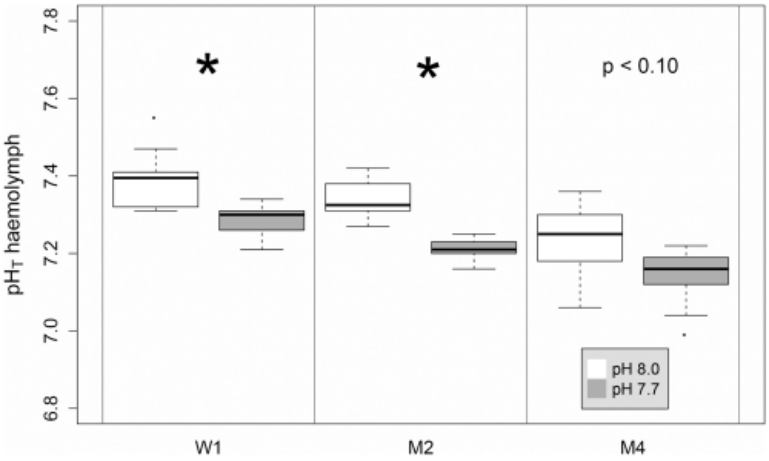

The phagocytosis efficiency was 33.3 ± 3.8 and 31.9 ± 3.8% at W1, 33.6 ± 3.6 and 38.4 ± 3.6% at M2, 13.9 ± 3.5 and 10.2 ± 3.5% at M4 for individuals exposed to pH 8.0 and pH 7.7, respectively. The phagocytosis efficiency of abalone haemocytes was not significantly impacted by low pH at W1, M2, and M4 (Table 3).

No significant difference in respiration or excretion rates was observed between the two pH treatments at any sampling time (Table 3). At the last point of measurement (M3), respiration rates were −3.29 ± 0.13 and −3.11 ± 0.12 µmol O_2 g^{-1} h^{-1} and excretion rates were 0.05 ± 0.06 and 0.02 ± 0.02 µmol NH_4 g^{-1} h^{-1}, respectively for individuals exposed to pH 8.0 and pH 7.7.

Gene expression

No significant difference in gene expression was observed between the two pH treatments for all tested genes at M4 (Table 3, Figure 4).

Figure 4. Expression pattern of Lustrin A, HSP71, HSP84, CA1, and CA2 genes in the mantle of adult abalone exposed to control (8.0, n = 16) and low (7.7, n = 14) pH for 4 months.

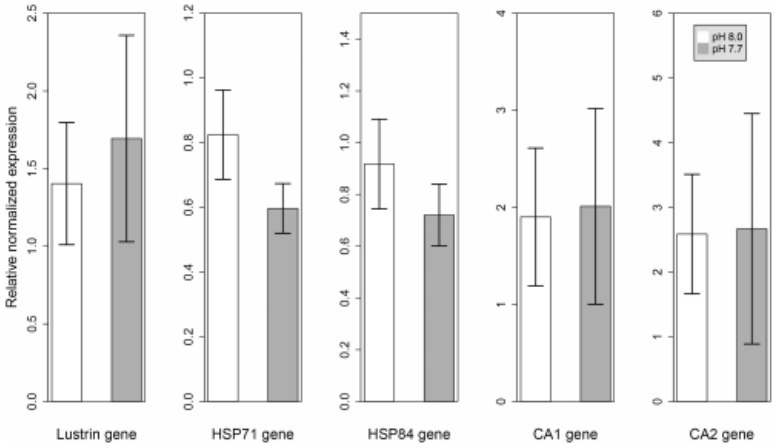

Shell pattern

Periostracum of abalone exposed to pH 7.7 was lighter than those exposed to pH 8.0 (Figure 5a and b). The periostracum of abalone exposed to low pH had a significantly paler colour than those of abalone exposed to pH 8.0, with darker colouration from M2 to M5 (Table 3, Figure 5c).

Figure 5. Shell colouration pattern of abalone after 5 months of exposure to (a) pH 8.0 and (b) pH 7.7 and (c) mean grey values (0: black to 255: white) of abalone shells exposed to two pH values (8.0 and 7.7, n = 10–39 per pH treatment) after 1 week (W1), and 2 (M2), 3 (M3), 4 (M4), and 5 (M5) months of exposure. Significant differences are indicated by * ($p < 0.05$, mixed model).

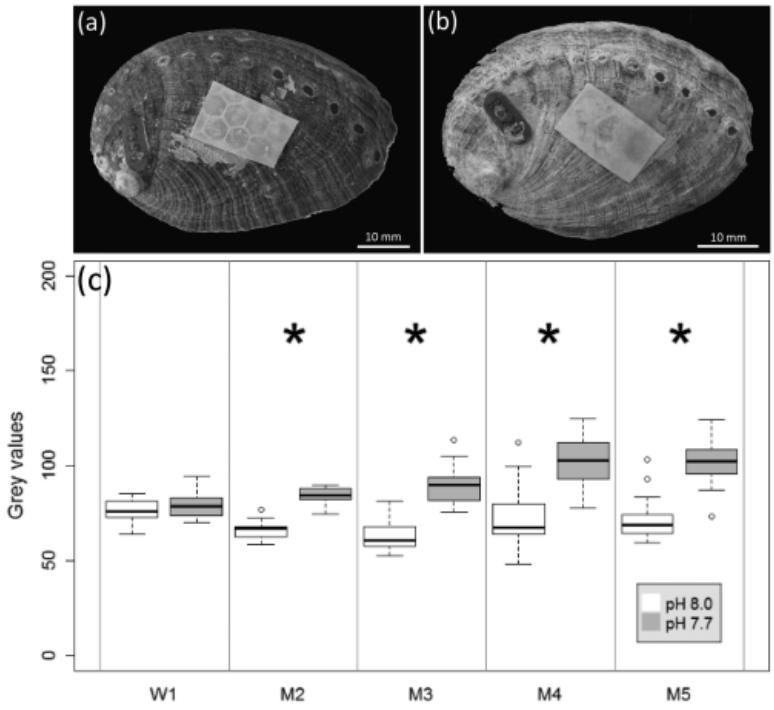

SEM examination of abalone shell surfaces exposed to pH 8.0 and pH 7.7 at M4 revealed differences in the texture and organization of outer and inner surface layers. The periostracum of control abalone (pH 8.0) had a homogeneous texture and regular organic sheets (Figure 6a and c). In contrast, the periostracum of individuals exposed to low pH (7.7) had an irregular and corroded surface (Figure 6b and d), revealing biominerals characteristic of the underlying spherulitic layer (Figure 6e).

Figure 6. SEM images of the outer shell surface of abalone grown in control conditions (pH 8.0, a, c) and under lower pH (pH 7.7, b, d, e) for 4 months. (a and b) Views of the shell border formed during the experiment. (c) Detail of the periostracum in the control, boxed in (a), showing a homogenous surface with the typical ridge and groove pattern. (d) Detail of the periostracum in the pH 7.7 treatment, showing the delamination of organic layer and revealing the underlying spherulitic layer. (e) Magnification of the corroded area boxed in (d) showing typical biominerals of the spherulitic layer.

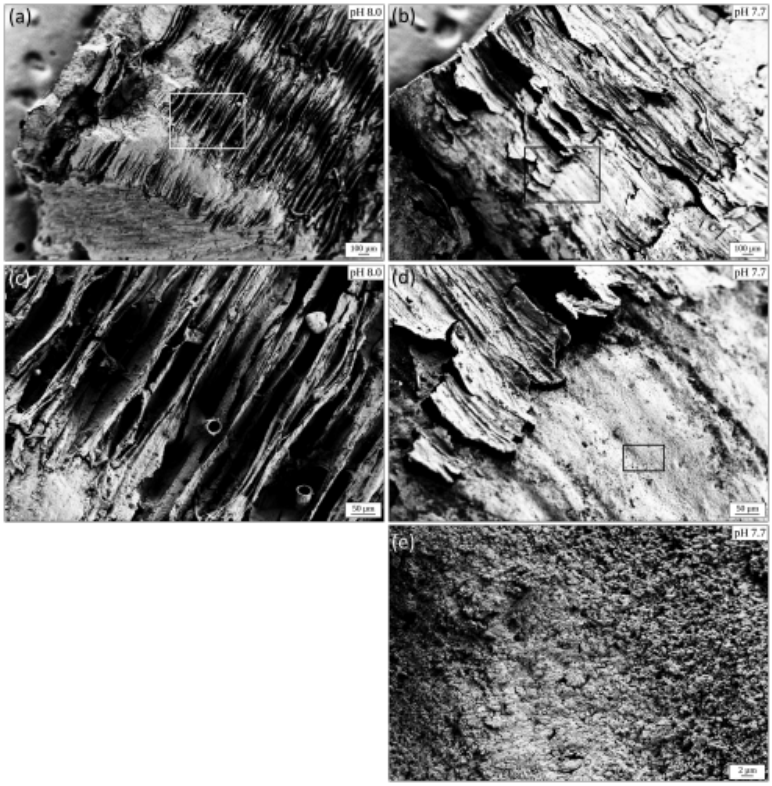

The inner nacreous layer showed a progressive maturation of aragonite platelets, forming a smooth homogeneous surface in individuals exposed to the two pH treatments (Figure 7a–d). At a higher magnification, the nacre growth region of control shell exhibited regular aragonite platelets joining progressively (Figure 7e). In abalone shell exposed to pH 7.7, the nacre surface of the growth region appeared corroded, with evidence of dissolution of the aragonite platelets (Figure 7f).

Figure 7. SEM images of the inner nacreous layer in control abalone shell (pH 8.0, a, c, e) and in abalone exposed to pH 7.7 for 4 months (b, d, f). (a and b) Inner nacreous layer showing a homogenous surface with growing aragonite platelets. (c and d) Magnification of the nacre growth region, boxed in (a) and (b), respectively. (e and f) Detail of the transition region between immature and mature nacre showing dissolution of the aragonite platelets under lower pH (f).

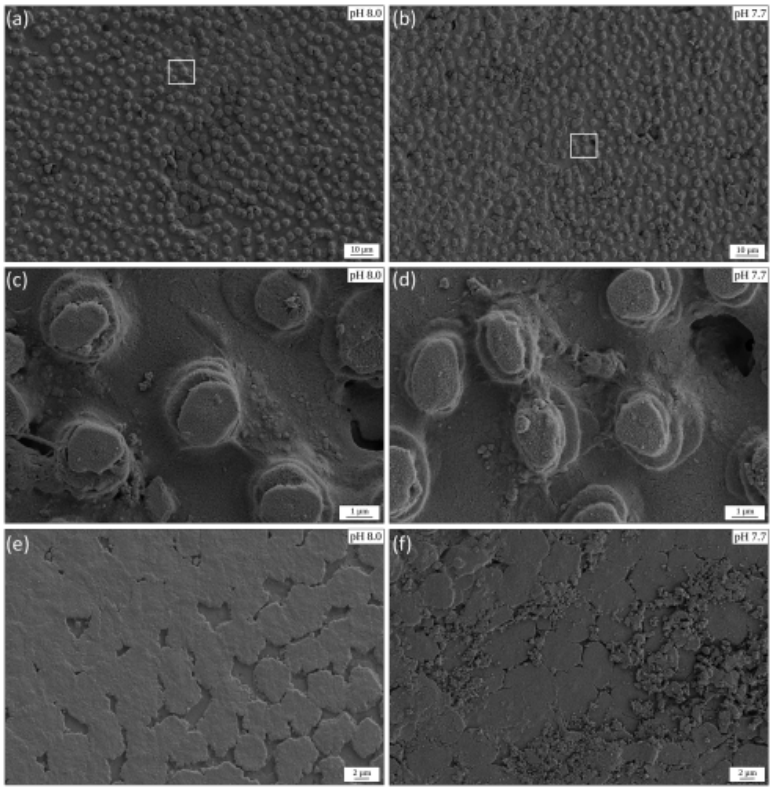

Shell calcification

Net calcification rate measured in individuals exposed to pH 7.7 was significantly lower than in those exposed to pH 8.0 at W1 and M3 (Table 3, Figure 8).

Figure 8. Net calcification rate of adult abalone exposed to two pH values (8.0 and 7.7, n = 9–15 per pH treatment) after 1 week (W1), and 2 (M2) and 3 (M3) months of exposure. Significant differences are indicated by * ($p < 0.05$, mixed model).

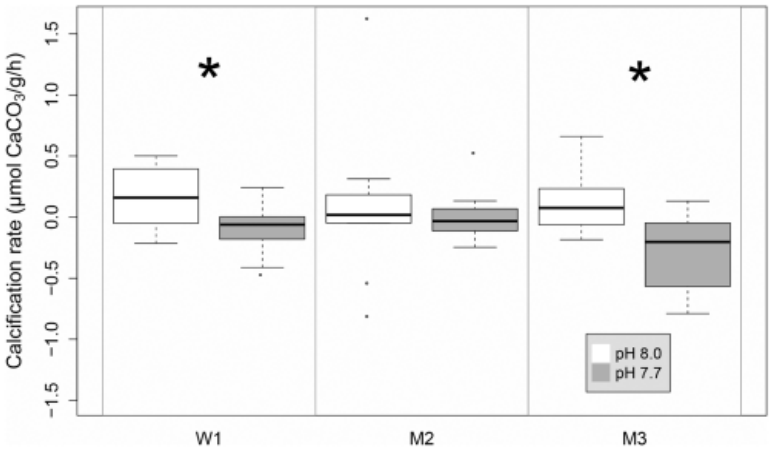

No significant differences were observed in shell weight and shell thickness between the two pH treatments at any sampling time (Table 3).

At M4, a significant thinner periostracum was observed for abalone exposed to pH 7.7 compared with those exposed to pH 8.0 (Table 3, Figure 9). The thickness of the spherulitic and nacre layers did not differ between the individuals exposed to the two pH treatments (Table 3, Figure 9).

Figure 9. Periostracum, spherulitic, and nacre layer thickness of adult abalone after 4 months of exposure to control (8.0, $n = 5$) and lowered (7.7, $n = 5$) pH. Significant difference is indicated by * ($p < 0.05$, mixed model).

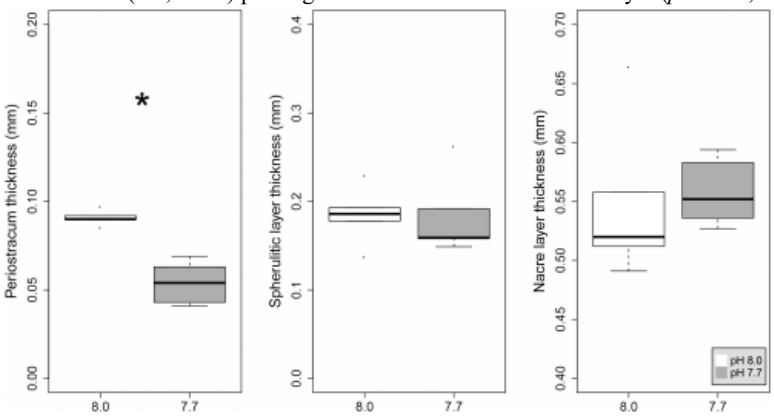

At M4, cross-sections in the newly formed shell (Figure 10a and b) revealed the distinction between the spherulitic and nacreous layers, both for individuals exposed to pH 8.0 (Figure 10c) and those exposed to pH 7.7 (Figure 10d). Magnification of the nacre platelets in cross-section revealed irregularities with a heterogeneous and corroded texture in the abalone exposed to pH 7.7 (Figure 10f) compared with those exposed to pH 8.0 (Figure 10e). In addition, the interspace between the aragonite platelets appeared reduced, resulting in a more tightly packed nacre layer in pH 7.7 (Figure 10e). No significant difference was observed in the thickness of nacreous tablets in the recent deposited nacre in abalone exposed to low pH at M4 compared with control abalone (0.42 ± 0.07 µm vs. 0.39 ± 0.07 µm respectively, Table 3); or in the older part of the shell (0.39 ± 0.03 µm vs. 0.44 ± 0.04 µm respectively, Table 3).

Figure 10. SEM images of shell cross-sections of adult abalone exposed to pH 8.0 (a, c, e) and 7.7 (b, d, f) for 4 months. (a and b) Cross-sections of the newly formed shell. (c and d) Detail of the interface between the spherulitic layer (sp) and the nacreous layer (n). (e) Magnification of the nacre layer boxed in (c) showing regular stacks of aragonite platelets. (f) Magnification of the nacre layer boxed in (d) showing pitting corrosion within the aragonite platelets at pH 7.7.

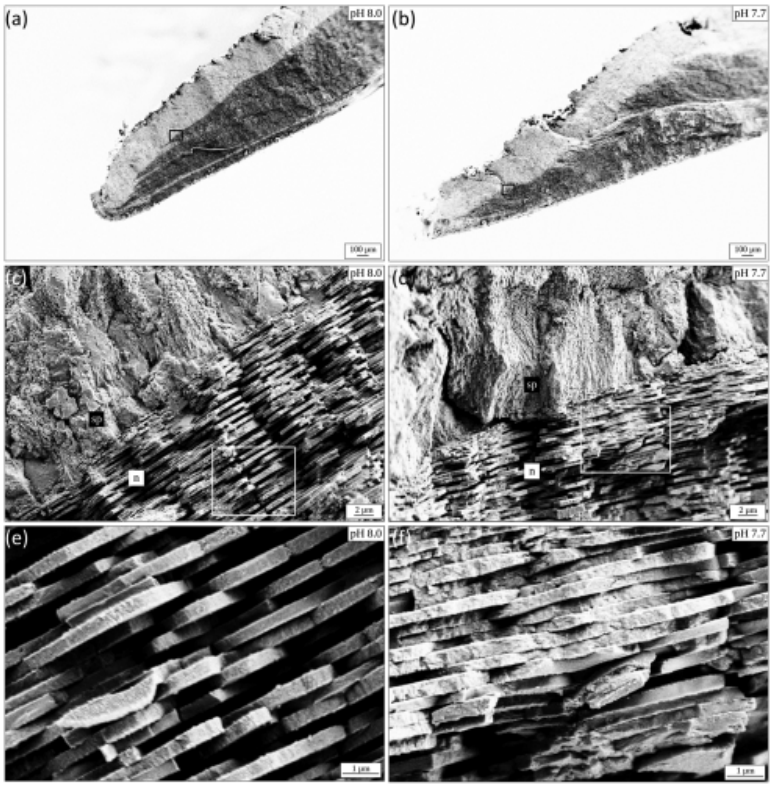

At M4, the shell fracture force was significantly lower for abalone shells exposed to pH 7.7 compared with the pH 8.0 control group (200 ± 70 N and 281 ± 71 N, respectively, Table 3). No linear relationship was found between the shell fracture force and shell length (linear regression, $R^2 = 0.037$, $F_{1,18} = 0.71$, $p = 0.412$), shell weight (linear regression, $R^2 = 0.130$, $F_{1,18} = 2.70$, $p = 0.118$), shell area (linear regression, $R^2 = 0.112$, $F_{1,17} = 2.15$, $p = 0.161$), or shell thickness (linear regression, $R^2 = 0.024$, $F_{1,16} = 0.39$, $p = 0.542$).

Weibull analysis of the characteristic Young's modulus E_0 obtained by nano-indentation revealed that Young's modulus of elasticity was significantly lower in the external layer than in the nacre (Supplementary Table S2). It also indicated that at pH 8.0 E_0 did not significantly differ according to zones (old, intermediate, newly formed) in the external layer and only slightly differed according to the zones in the nacre, the intermediate zone E_0 being significantly different from that of the old zone (Figure 11, Supplementary Table S2). On the contrary, under low pH, the E_0 values differed significantly according to zone (Figure 11, Supplementary Table S2). Furthermore, the analysis revealed that the shells of abalone exposed to low pH had a lower Young's modulus of elasticity. This was true for each layer (external layer and nacre) and for each zone (old, intermediate, and newly formed) with the exception of the old zone of the external layer whose E_0 did not differ according to pH (Figure 11, Supplementary Table S2).

Figure 11. Nano-indentation measures of hardness (H0) and Young's modulus of elasticity (E0) in the external layer and in the nacre of abalone shell exposed to two pH values (8.0 and 7.7) for 4 months ($n = 4$ per pH treatment). O, I, and N refer to the shell regions investigated, i.e. O, old; I, intermediate; and N, new part of the shell. Weibull analysis was used to calculate the 95% confidence intervals of E0 and H0 corresponding to 63% of the population with the modified least square regression according to Bütikofer *et al.* (2015).

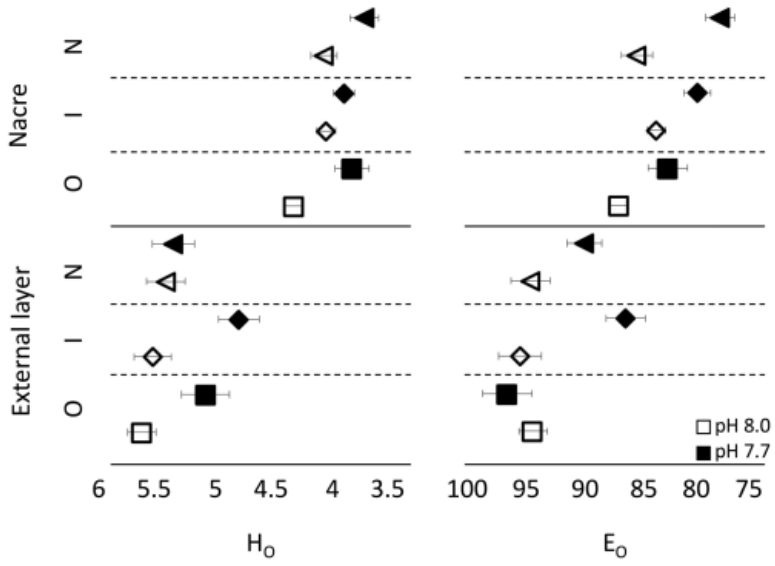

Weibull analysis of characteristic nano-hardness (H_0) revealed similar changes as for E_0. At pH 8.0, H_0 did not differ according to zones in the external layer and was only slightly (but significantly) higher in the old nacre zone than in the two other zones of this layer. H_0 was significantly lower at pH 7.7 than at pH 8.0, except in the newly formed zone of the external layer and in the intermediate layer of the nacre (Figure 11, Supplementary Table S3).

Discussion

This study used a multifactorial approach to investigate several biological (including survival and growth reported as length), physiological (including pH_T of haemolymph, gene expression relating to calcification, and metabolic rates), and structural (including shell strength, nano-indentation measurements, and SEM imaging of microstructure) responses in adult abalone *H. tuberculata* exposed to decreased pH. A number of biological parameters involved in shell calcification, as growth, shell strength or microstructure, and acid-base regulation, as pH_T of haemolymph, was reduced at pH 7.7, while survival, metabolism, and haemocyte phagocytosis were not significantly affected.

A significant effect of OA was observed on several biological responses including shell growth of adult abalone in terms of length after 5 months of low pH exposure, which is in accordance with previous studies on juvenile abalone. Indeed, Cunningham *et al.* (2016) reported significant reductions in shell length and weight in juveniles *Haliotis iris* exposed to low pH (−0.3 to −0.5 pH units from ambient pH). Similarly, reduced shell growth in length under acidified pH conditions has recently been reported in 6-month-old juvenile *H. tuberculata* exposed to pH 7.6 (Auzoux-Bordenave *et al.*, 2019). Although there are no studies available on adult abalone, our results are consistent with previous research showing a shell growth reduction in almost all mollusc taxa exposed to OA (Gazeau *et al.*, 2013; Kroeker *et al.*, 2013) but with differences according to life stage. For example, adult snails *Nucella lamellosa* exposed to acidified conditions (−0.2 and −0.4 pH units from ambient pH) showed a decline in shell growth due to an increased dissolution of shell material (Nienhuis *et al.*, 2010). Significant growth reductions are regularly observed in juveniles exposed to acidified conditions (Michaelidis *et al.*, 2005; Beniash *et al.*, 2010; Thomsen and Melzner, 2010; Amaral *et al.*, 2012), but the magnitude of the effect is generally smaller in adults, where the calcification is lower.

In adult *H. tuberculata*, no significant differences in shell weight and shell thickness were found between the two pH treatments. However, after 4 months under low pH exposure, abalone shells showed a corroded and disorganized periostracum, which was associated to changes in shell coloration. The periostracum plays a role in maintaining shell integrity in acidified seawater conditions (Ries *et al.*, 2009), protecting individuals from dissolution in $CaCO_3$-undersaturated waters (Hüning *et al.*, 2013). In our study, the periostracum appeared clearly corroded under lower pH, showing biominerals emerging from the underlying spherulitic layer. This was confirmed by a significant reduction of the periostracum thickness. These observations are consistent with previous observations relating prominent dissolution on the outer surface of juvenile abalone and other mollusc shells (McClintock *et al.*, 2009; Meng *et al.*, 2018; Auzoux-Bordenave *et al.*, 2019). In addition, corrosion of aragonite platelets and surface dissolution was observed

within the nacreous inner layer of the shell from individuals exposed to pH 7.7. No significant differences were observed in the thickness of the spherulitic layer, which is just beneath the periostracum. As previously seen in juvenile stage of *H. tuberculata* (Auzoux-Bordenave *et al.*, 2019), these observations suggest a reduction in shell protection from environmental disturbances and also from potential predators in adult abalone.

Although no significant differences in nacre thickness were found, the decrease of −0.3 pH units resulted in a partial dissolution of nacreous surface. The nacre surface dissolution is consistent with the effects observed on juvenile abalone and adult bivalve shells grown at similar levels of pH treatments (McClintock *et al.*, 2009; Thomsen *et al.*, 2010; Welladsen *et al.*, 2010; Melzner *et al.*, 2011; Auzoux-Bordenave *et al.*, 2019). In juvenile *Mytilus edulis*, the aragonite layer was more vulnerable than the calcite layer under low pH (−0.8 pH units from ambient), with a corroded and dissolved surface (Thomsen *et al.*, 2010; Melzner *et al.*, 2011). The growth of new nacre tablets was also disrupted in adult pearl oysters *Pinctada fucata* kept at pH 7.6, as the developing tablets were deformed and irregular (Welladsen *et al.*, 2010). In *H. tuberculata* nacre, we also evidenced a reduction of the inter-tabular space within the aragonite platelets, resulting in a more tightly packed nacre layer in pH 7.7. The tight packing of nacre platelets under lower pH suggests changes in the structural organization of organic matrix surrounding the platelets. This might be further explored by combining high-resolution TEM and electron energy loss spectroscopy to gain local information and detect fine changes in the organo-mineral interface.

In *H. tuberculata*, the main $CaCO_3$ polymorph composing the shell is aragonite (Auzoux-Bordenave *et al.*, 2010; Auzoux-Bordenave *et al.*, 2015), indicating that this species is more susceptible to dissolution than other mollusc shells composed of only calcite or a mixture of calcite/aragonite (Gazeau *et al.*, 2013; Parker *et al.*, 2013). The formation of calcified layers is strongly impacted when the saturation state of aragonite in seawater is <1 (Comeau *et al.*, 2010; Gazeau *et al.*, 2013). Since the aragonite saturation state ($\Omega_{aragonite}$) of the seawater was always >1 in our study, the shell effects might not be entirely due to shell dissolution. It is suggested that indirect metabolic effects, such as disruption of the acid-base balance, would be partly responsible for shell corrosion and microstructure changes observed under lower pH. In our study, net calcification of adult abalone was significantly decreased at lower pH (7.7), which is a common response in molluscs (Beniash *et al.*, 2010; Range *et al.*, 2011; Melatunan *et al.*, 2013). Indeed, previous studies on temperate bivalves exposed to acidified seawater have shown reduced calcification rates that would compromise the structural integrity of the shell (Michaelidis *et al.*, 2005; Gazeau *et al.*, 2007; Ries *et al.*, 2009; Beniash *et al.*, 2010; Range *et al.*, 2011). On adult slipper limpet, *Crepidula fornicata*, negative calcification rates in individuals exposed to very low pH (−0.5 pH units) were correlated with a degraded periostracum and/or physiological changes (Noisette *et al.*, 2016). The alteration of the periostracum and corrosion of the nacreous layer observed in abalone shells may be partly explained by a reduced calcification rate.

Previous experimental studies on OA reported that a reduction in shell structural integrity induced significant reduction in mechanical properties (Beniash *et al.*, 2010; Dickinson *et al.*, 2012; Fitzer *et al.*, 2015). Our study investigated for the first time the impacts of OA on the biomechanical properties of adult abalone shell. The shell fracture force was significantly reduced after 4 months of exposure to acidified seawater. This result is consistent with the changes in shell microstructure observed under SEM. In juvenile *H. tuberculata* shell, the reduction of shell fracture force under low pH (pH 7.6) resulted from both reduced growth and shell dissolution (Auzoux-Bordenave *et al.*, 2019). At the adult stage, the fracture force of abalone shells exposed to pH 7.7 was reduced by 29% compared with the control, indicating that defects induced by OA in adult shells are more severe than those induced in the juvenile ones. Indeed, significantly lower elasticity and hardness were observed in the newly formed shell of abalone exposed to acidified seawater. In contrast, values for the oldest part of the shell were similar to those recorded in the shells of abalone exposed to pH 8.0. This suggests that the synthesis of new shell is the affected process, rather than corrosion (which impacted the whole shell surface). These results also indicate that the material properties themselves are affected in both the nacre and spherulitic layers and that this induced mechanical weakness of the shell. Similar results were reported in *M. edulis* (Fitzer *et al.*, 2015) but this is, to our knowledge, the first evidence in gastropods, suggesting that the shell formation process is affected differently among mollusc clades.

Along with direct impacts on calcification, exposure to low pH seawater may also have indirect effects on the extracellular acid-base equilibrium, leading to general internal acidosis, changes in energy balance and disruption in shell calcification (Pörtner *et al.*, 2004; Melzner *et al.*, 2009; Waldbusser *et al.*, 2011). The multifactorial approach used in this study also allowed the assessment of acid-base, metabolism, and physiology parameters in adult abalone

H. tuberculata facing OA. A decrease in haemolymph pH was observed under lower pH during the first 2 months of exposure, indicating a lack of compensation in abalone facing OA. Elevated H^+ concentration and subsequent changes in acid-base balance would likely be responsible for the reduction of shell calcification in marine molluscs (Waldbusser *et al.*, 2011; Cyronak *et al.*, 2016). Furthermore, an increased cost for ion regulation combined with decreased growth could lead to a lower rate of calcification (Pörtner *et al.*, 2004; Michaelidis *et al.*, 2005). In the present study, we demonstrated that adult *H. tuberculata* do not compensate for a seawater pH decrease of 0.3 pH units, suggesting that changes in the extracellular balance might be partly responsible for the alteration of shell integrity.

Among the physiological processes involved in shell calcification, matrix protein production and specific enzymatic activities (i.e. CA) have been shown to be influenced by decreased pH (Weiss *et al.*, 2013). Our study also investigated the expression of five genes involved in abalone shell biomineralization (Lustrin A, CA1, and CA2) and stress response (HSP70 and HSP84). Despite evidence of shell damage, no difference was found in the expression of the biomineralization genes nor in genes involved in stress responses. The activity of CA, which plays a major role in the formation of carbonate ions, was significantly reduced in adult *M. edulis* exposed to a similar pH decrease (Fitzer *et al.*, 2014). However, in this study, only CA activity was measured and gene expression was not evaluated. An increase of HSP gene expression has been previously reported in mollusc exposed either to thermal stress (Farcy *et al.*, 2007) or to lower pH (Cummings *et al.*, 2011). In the present study on *H. tuberculata*, we did not find any change in the expression of target genes, suggesting that the physiological responses to OA would occur at another level of regulation such as protein synthesis or structural organization. As already performed in *Haliotis rufescens* (De Wit and Palumbi, 2013), future works would likely include a complete transcriptome analysis in the mantle of *H. tuberculata* in order to identify the molecular responses of European abalone to OA.

OA may also impact the physiological status and functionality of the haemocytes, as previously shown in *M. edulis* (Bibby *et al.*, 2008). In adult abalone *H. tuberculata*, the immune response, evaluated by haemocyte phagocytosis, was not significantly affected by lowered pH, regardless of the sampling time. In addition, no significant changes were observed in global metabolism (respiration and excretion rates) between animals in the control treatment and those at lowered pH. This is consistent with previous results on calcifying molluscs showing that metabolism was only slightly increased among adult individuals (reviewed in Kroeker *et al.*, 2013). The absence of significant effects on abalone metabolism is also in accordance with the results obtained on juvenile *H. iris* (Cunningham *et al.*, 2016) and adult *C. fornicata* (Noisette *et al.*, 2016). The capacity of abalone to grow under future pH conditions will depend on their potential to maintain their vital functions. Since the seawater pH along the Brittany coast naturally varies from 7.9 to 8.2 (Legrand *et al.*, 2018; Qui-Minet *et al.*, 2018), the experimental scenario testing a decrease of −0.3 units from ambient pH is consistent with natural variations experienced by abalone in the tidal zone.

From these results, it was concluded that European abalone *H. tuberculata* did not compensate the decrease of seawater pH (−0.3 pH units) during the first 2 months of exposure, but started to acclimate after 4 months, as suggested by the compensation of their extracellular pH. After 4 months of exposure under low pH, the acid-base balance and global metabolism were not affected by OA but occurred at a cost to shell growth and structural integrity. Indeed, adverse effects on shell growth, calcification, and mechanical properties were observed, supporting the idea that OA altered the biomineral architecture and lead to more fragile shell. These effects are of particular concern in this economically and ecologically important abalone species. The decrease in shell resistance might reduce protection from predators and potentially impact wild abalone populations already threatened by overfishing and environmental perturbations (Cook, 2016). This effect adds to the increased mortality and reduced growth already reported in larvae and juvenile of *H. tuberculata* for pH of 7.6 (Wessel *et al.*, 2018; Auzoux-Bordenave *et al.*, 2019). Because abalone are slow-growing species, the impact of a decreased pH during the aquaculture cycle might substantially increase production costs by increasing the time necessary for animals to reach a marketable size.

Supplementary data

Supplementary material is available at the *ICESJMS* online version of the manuscript.

Acknowledgements[AQ9]

This work was supported in part by the ATM program “Abalone shell mineralization” of the MNHN funded by the *Ministère délégué à l’Enseignement Supérieur et à la Recherche* (Paris, France), the program “Acidification des Océans” (ICOBio project) funded by the *Fondation pour la Recherche sur la Biodiversité* (FRB) and the *Ministère de*

la Transition Ecologique et Solidaire (MTES), and the French LabexMER program (OASYS project). SA was supported by a post-doctoral fellowship from the MNHN funded by the *Ministère de la Transition Ecologique et Solidaire* (MTES). SDG is holder of a FRIA PhD fellowship from the National Fund for Scientific Research (NFSR, Belgium) and PhD is a Research Director of the NFSR. The Regional Council of Brittany, the General Council of Finistère, the urban community of Concarneau Cornouaille Agglomération, and the European Regional Development Fund (ERDF) are acknowledged for the funding of the scanning electron microscope (Sigma 300 FE-SEM) at the Concarneau Marine Station. We thank Stéphane Formosa for his assistance in SEM (*Plateau technique de Microscopie Electronique du Muséum National d'Histoire Naturelle*, Concarneau, France). We are grateful to Olivier Mouchel for his help in sampling abalone and Nicolas Brodu who participated to the experimental work and biological analyses during his master training. We thank all the staff of the France Haliotis farm (Plouguerneau) for hosting the experiment. Finally, we thank the Translation Bureau of the University of Western Brittany for improving the English of this manuscript.

Authors' contributions[AQ10]

SA-B, SM, SR, and PD designed the experiment; MC, SR, AB, and SH performed the experiment; SH provided the facilities; NR, SDG, LM, and PD performed the mechanical analysis and the data analysis; AS and FG performed the gene expression analysis; SA, SR, and SA-B analysed the data and wrote the main paper. All authors discussed the results and implications and commented on the manuscript at all stages.

References

Amaral, V., Cabral, H., and Bishop, M. 2012. Moderate acidification affects growth but not survival of 6-month-old oysters. Aquatic Ecology, 46: 119–127.

Auzoux-Bordenave, S., Badou, A., Gaume, B., Berland, S., Helléouet, M. N., Milet, C., and Huchette, S. 2010. Ultrastructure, chemistry and mineralogy of the growing shell of the European abalone *Haliotis tuberculata*. Journal of Structural Biology, 171: 277–290.

Auzoux-Bordenave, S., Brahmi, C., Badou, A., De Rafélis, M., and Huchette, S. 2015. Shell growth, microstructure and composition over the development cycle of the European abalone *Haliotis tuberculata*. Marine Biology, 162: 687–697.

Auzoux-Bordenave, S., Wessel, N., Badou, A., Martin, S., M'Zoudi, S., Avignon, S., Roussel, S., et al. 2019. Ocean acidification impacts growth and shell mineralization in juvenile abalone (*Haliotis tuberculata*). Marine Biology, in press.[AQ11]

Beniash, E., Ivanina, A., Lieb, N. S., Kurochkin, I., and Sokolova, I. M. 2010. Elevated level of carbon dioxide affects metabolism and shell formation in oysters *Crassostrea virginica*. Marine Ecology Progress Series, 419: 95–108.

Bibby, R., Widdicombe, S., Parry, H., Spicer, J., and Pipe, R. 2008. Effects of ocean acidification on the immune response of the blue mussel *Mytilus edulis*. Aquatic Biology, 2: 67–74.

Bütikofer, L., Stawarczyk, B., and Roos, M. 2015. Two regression methods for estimation of a two-parameter Weibull distribution for reliability of dental materials. Dental Materials, 31: e33–e50.

Cadiz, L., Servili, A., Quazuguel, P., Madec, L., Zambonino-Infante, J.-L., and Mazurais, D. 2017. Early exposure to chronic hypoxia induces short- and long-term regulation of hemoglobin gene expression in European sea bass (*Dicentrarchus labrax*). The Journal of Experimental Biology, 220: 3119–3126.

Caldeira, K., and Wickett, M. E. 2003. Anthropogenic carbon and ocean pH. Nature, 425: 365.

Comeau, S., Gorsky, G., Alliouane, S., and Gattuso, J. P. 2010. Larvae of the pteropod *Cavolinia inflexa* exposed to aragonite undersaturation are viable but shell-less. Marine Biology, 157: 2341–2345.

Cook, P. A. 2016. Recent trends in worldwide abalone production. Journal of Shellfish Research, 35: 581–583.

Cummings, V., Hewitt, J., Van Rooyen, A., Currie, K., Beard, S., Thrush, S., Norkko, J., et al. 2011. Ocean acidification at high latitudes: potential effects on functioning of the antarctic bivalve *Laternula elliptica*. PLoS One, 6. [AQ12]

Cunningham, S. C., Smith, A. M., and Lamare, M. D. 2016. The effects of elevated pCO_2 on growth, shell production and metabolism of cultured juvenile abalone, *Haliotis iris*. Aquaculture Research, 47: 2375–2392.

Cyronak, T., Schulz, K. G., and Jokiel, P. L. 2016. The Omega myth: what really drives lower calcification rates in an acidifying ocean. ICES Journal of Marine Science, 73: 558–562.

De Wit, P., and Palumbi, S. R. 2013. Transcriptome-wide polymorphisms of red abalone (*Haliotis rufescens*) reveal patterns of gene flow and local adaptation. Molecular Ecology, 22: 2884–2897.

Dickinson, G. H., Ivanina, A. V., Matoo, O. B., Portner, H. O., Lannig, G., Bock, C., Beniash, E., et al. 2012. Interactive effects of salinity and elevated CO_2 levels on juvenile eastern oysters, *Crassostrea virginica*. Journal of Experimental Biology, 215: 29–43.

Dickson, A. G. 2010. Standards for ocean measurements. Oceanography, 23: 34–47.

Dickson, A. G., and Millero, F. J. 1987. A comparison of the equilibrium constants for the dissociation of carbonic acid in seawater media. Deep-Sea Research, 34: 1733–1743.

Dickson, A. G., Sabine, C. L., and Christian, J. R. (Eds). 2007. Guide to Best Practices for Ocean CO_2 Measurements. PICES Special Publication. 191 pp.[AQ13]

Fabry, V. J. 2008. Marine calcifiers in a high-CO_2 ocean. Science, 320: 1020–1022.

Farcy, E., Serpentini, A., Fiévet, B., and Lebel, J.-M. 2007. Identification of cDNAs encoding HSP70 and HSP90 in the abalone *Haliotis tuberculata*: transcriptional induction in response to thermal stress in hemocyte primary culture. Comparative Biochemistry and Physiology Part B: Biochemistry and Molecular Biology, 146: 540–550.

Fitzer, S. C., Phoenix, V. R., Cusack, M., and Kamenos, N. A. 2014. Ocean acidification impacts mussel control on biomineralisation. Scientific Reports, 4: 6218.

Fitzer, S. C., Zhu, W., Tanner, K. E., Phoenix, V. R., Kamenos, N. A., and Cusack, M. 2015. Ocean acidification alters the material properties of *Mytilus edulis* shells. Journal of the Royal Society Interface, 12.

Gattuso, J. P., Magnan, A., Bille, R., Cheung, W. W. L., Howes, E. L., Joos, F., Allemand, D., et al. 2015. Contrasting futures for ocean and society from different anthropogenic CO_2 emissions scenarios. Science, 349: aac4722.

Gaume, B., Denis, F., Van Wormhoudt, A., Huchette, S., Jackson, D. J., Avignon, S., and Auzoux-Bordenave, S. 2014. Characterisation and expression of the biomineralising gene Lustrin A during shell formation of the European abalone *Haliotis tuberculata*. Comparative Biochemistry and Physiology Part B: Biochemistry and Molecular Biology, 169: 1–8.

Gazeau, F., Parker, L. M., Comeau, S., Gattuso, J.-P., O'Connor, W. A., Martin, S., Pörtner, H.-O., et al. 2013. Impacts of ocean acidification on marine shelled molluscs. Marine Biology, 160: 2207–2245.

Gazeau, F., Quiblier, C., Jansen, J. M., Gattuso, J.-P., Middelburg, J. J., and Heip, C. H. R. 2007. Impact of elevated CO_2 on shellfish calcification. Geophysical Research Letters, 34: L07703.

Hendriks, I. E., Duarte, C. M., and Álvarez, M. 2010. Vulnerability of marine biodiversity to ocean acidification: a meta-analysis. Estuarine, Coastal and Shelf Science, 86: 157–164.

Hoegh-Guldberg, O., Mumby, P. J., Hooten, A. J., Steneck, R. S., Greenfield, P., Gomez, E., Harvell, C. D., et al. 2007. Coral reefs under rapid climate change and ocean acidification. Science, 318: 1737–1742.

Hofmann, G. E., Barry, J. P., Edmunds, P. J., Gates, R. D., Hutchins, D. A., Klinger, T., and Sewell, M. A. 2010. The effect of ocean acidification on calcifying organisms in marine ecosystems: an organism-to-ecosystem perspective. Annual Review of Ecology, Evolution and Systematics, 41: 127–147.

Huchette, S., and Clavier, J. 2004. Status of the ormer (*Haliotis tuberculata* L.) industry in Europe. Journal of Shellfish Research, 23: 951–955.

Hüning, A. K., Melzner, F., Thomsen, J., Gutowska, M. A., Krämer, L., Frickenhaus, S., Rosenstiel, P., et al. 2013. Impacts of seawater acidification on mantle gene expression patterns of the Baltic Sea blue mussel: implications for shell formation and energy metabolism. Marine Biology, 160: 1845–1861.

IPCC. 2014. Summary for Policymakers. *In* Climate Change 2014: Impacts, Adaptation, and Vulnerability. Part A: Global and Sectoral Aspects. Contribution of Working Group II to the Fifth Assessment Report of the Intergovernmental Panel on Climate Change, pp. 1–32. Cambridge University Press, Cambridge, UK and New York, NY.[AQ14]

Kroeker, K. J., Kordas, R. L., Crim, R., Hendriks, I. E., Ramajo, L., Singh, G. S., Duarte, C. M., et al. 2013. Impacts of ocean acidification on marine organisms: quantifying sensitivities and interaction with warming. Global Change Biology, 19: 1884–1896.

Kuznetsova, A., Brockhoff, P. B., and Christensen, R. H. B. 2017. lmerTest package: tests in linear mixed effects models. Journal of Statistical Software, 82: 1–26.

Le Roy, N., Marie, B., Gaume, B., Guichard, N., Delgado, S., Zanella-Cléon, I., Becchi, M., et al. 2012. Identification of two carbonic anhydrases in the mantle of the European abalone *Haliotis tuberculata* (Gastropoda, Haliotidae): phylogenetic implications. Journal of Experimental Zoology Part B: Molecular and Developmental Evolution, 318: 353–367.

Legrand, E., Riera, P., Pouliquen, L., Bohner, O., Cariou, T., and Martin, S. 2018. Ecological characterization of intertidal rockpools: seasonal and diurnal monitoring of physico-chemical parameters. Regional Studies in Marine Science, 17: 1–10.

Marchant, H. K., Calosi, P., and Spicer, J. I. 2010. Short-term exposure to hypercapnia does not compromise feeding, acid–base balance or respiration of *Patella vulgata* but surprisingly is accompanied by radula damage. Journal of the Marine Association of the United Kingdom, 90: 1379–1384.

McClintock, J. B., Angus, R. A., Mcdonald, M. R., Amsler, C. D., Catledge, S. A., and Vohra, Y. K. 2009. Rapid dissolution of shells of weakly calcified Antarctic benthic macroorganisms indicates high vulnerability to ocean acidification. Antarctic Science, 21: 449–456.

Mehrbach, C., Culberson, C. H., Hawley, J. E., and Pytkowicx, R. M. 1973. Measurement of the apparent dissociation constants of carbonic acid in seawater at atmospheric pressure. Limnology and Oceanography, 18: 897–907.

Melatunan, S., Calosi, P., Rundle, S., Widdicombe, S., and Moody, A. 2013. Effects of ocean acidification and elevated temperature on shell plasticity and its energetic basis in an intertidal gastropod. Marine Ecology Progress Series, 472: 155–168.

Melzner, F., Gutowska, M. A., Langenbuch, M., Dupont, S., Lucassen, M., Thorndyke, M. C., Bleich, M., et al. 2009. Physiological basis for high CO_2 tolerance in marine ectothermic animals: pre-adaptation through lifestyle and ontogeny? Biogeosciences, 6: 2313–2331.

Melzner, F., Stange, P., Trübenbach, K., Thomsen, J., Casties, I., Panknin, U., Gorb, S. N., et al. 2011. Food supply and seawater pCO_2 impact calcification and internal shell dissolution in the blue mussel *Mytilus edulis*. PLoS One, 6: e24223.

Meng, Y., Guo, Z., Fitzer, S. C., Upadhyay, A., Chan, V. B. S., Li, C., Cusack, M., et al. 2018. Ocean acidification reduces hardness and stiffness of the Portuguese oyster shell with impaired microstructure: a hierarchical analysis. Biogeosciences, 15: 6833–6846.

Michaelidis, B., Ouzounis, C., Paleras, A., and Pörtner, H.-O. 2005. Effects of long-term moderate hypercapnia on acid–base balance and growth rate in marine mussels *Mytilus galloprovincialis*. Marine Ecology Progress Series, 293: 109–118.

Morash, A. J., and Alter, K. 2015. Effects of environmental and farm stress on abalone physiology: perspectives for abalone aquaculture in the face of global climate change. Reviews in Aquaculture, 7: 1–27.

Morse, J. W., Arvidson, R. S., and Lüttge, A. 2007. Calcium carbonate formation and dissolution. Chemical Reviews, 107: 342–381.

Nienhuis, S., Palmer, A. R., and Harley, C. D. G. 2010. Elevated CO_2 affects shell dissolution rate but not calcification rate in a marine snail. Proceedings of the Royal Society B: Biological Sciences, 277: 2553–2558.

Noisette, F., Bordeyne, F., Davoult, D., and Martin, S. 2016. Assessing the physiological responses of the gastropod *Crepidula fornicata* to predicted ocean acidification and warming. Limnology and Oceanography, 61: 430–444.

Orr, J. C., Fabry, V. J., Aumont, O., Bopp, L., Doney, S. C., Feely, R. A., Gnanadesikan, A., et al. 2005. Anthropogenic ocean acidification over the twenty-first century and its impact on calcifying organisms. Nature, 437: 681–686.

Parker, L., Ross, P., O'Connor, W., Pörtner, H., Scanes, E., and Wright, J. 2013. Predicting the response of molluscs to the impact of ocean acidification. Biology, 2: 651–692.

Parker, L. M., Ross, P. M., O'Connor, W. A., Borysko, L., Raftos, D. A., and Pörtner, H.-O. 2012. Adult exposure influences offspring response to ocean acidification in oysters. Global Change Biology, 18: 82–92.

Pierrot, D. E., Lewis, E., and Wallace, D. W. R. 2006. MS Excel Program Developed for CO_2 System Calculations. ORNL/CDIAC-105a. Carbon Dioxide Information Analysis Center. Oak Ridge National Laroratory, US Department of Energy, Oak Ridge, TN.

Pörtner, H. O., Langenbuch, M., and Reipschläger, A. 2004. Biological impact of elevated ocean CO_2 concentrations: lessons from animal physiology and earth history. Journal of Oceanography, 60: 705–718.

Qui-Minet, Z. N., Delaunay, C., Grall, J., Six, C., Cariou, T., Bohner, O., Legrand, E., et al. 2018. The role of local environmental changes on maerl and its associated non-calcareous epiphytic flora in the Bay of Brest. Estuarine, Coastal and Shelf Science, 208: 140–152.

R Core Team. 2015. R Core Team: A language and environment for statistical computing. Vienna, Austria. https://www.R-project.org/[AQ15]

Range, P., Chícharo, M. A., Ben-Hamadou, R., Piló, D., Matias, D., Joaquim, S., Oliveira, A. P., et al. 2011. Calcification, growth and mortality of juvenile clams *Ruditapes decussatus* under increased pCO_2 and reduced pH: variable responses to ocean acidification at local scales? Journal of Experimental Marine Biology and Ecology, 396: 177–184.

Ries, J. B., Cohen, A. L., and McCorkle, D. C. 2009. Marine calcifiers exhibit mixed responses to CO_2-induced ocean acidification. Geology, 37: 1131–1134.

Rogers-Bennett, L. 2007. Is climate change contributing to range reductions and localized extinctions in northern (*Haliotis kamtschatkana*) and flat (*Haliotis walallensis*) abalones? Bulletin of Marine Science, 81: 283–296.

Sabine, C. L., Feely, R. A., Gruber, N., Key, R. M., Lee, K., Bullister, J. L., Wanninkhof, R., et al. 2004. The oceanic sink for anthropogenic CO_2. Science, 305: 367–371.

Shen, X., Belcher, A. M., Hansma, P. K., Stucky, G. D., and Morse, D. E. 1997. Molecular cloning and characterization of Lustrin A, a matrix protein from shell and pearl nacre of *Haliotis rufescens*. The Journal of Biological Chemistry, 272: 32472–32481.

Smith, S. V., and Key, G. S. 1975. Carbon dioxide and metabolism in marine environments. Limnology and Oceanography, 20: 493–495.

Solorzano, L. 1969. Determination of ammonia in natural waters by the phenolhypochlorite method. Limnology and Oceanography, 14: 799–801.

Thomsen, J., Gutowska, M. A., Saphörster, J., Heinemann, A., Trübenbach, K., Fietzke, J., Hiebenthal, C., et al. 2010. Calcifying invertebrates succeed in a naturally CO_2-rich coastal habitat but are threatened by high levels of future acidification. Biogeosciences, 7: 3879–3891.

Thomsen, J., and Melzner, F. 2010. Moderate seawater acidification does not elicit long-term metabolic depression in the blue mussel *Mytilus edulis*. Marine Biology, 157: 2667–2676.

Travers, M.-A., Basuyaux, O., Le Goic, N., Huchette, S., Nicolas, J.-L., Koken, M., and Paillard, C. 2009. Influence of temperature and spawning effort on *Haliotis tuberculata* mortalities caused by *Vibrio harveyi*: an example of emerging vibriosis linked to global warming. Global Change Biology, 15: 1365–1376.

Travers, M.-A., Mirella da Silva, P., Le Goïc, N., Marie, D., Donval, A., Huchette, S., Koken, M., et al. 2008. Morphologic, cytometric and functional characterisation of abalone (*Haliotis tuberculata*) haemocytes. Fish & Shellfish Immunology, 24: 400–411.

Vilchis, L. I., Tegner, M. J., Moore, J. D., Friedman, C. S., Riser, K. L., Robbins, T. T., and Dayton, P. K. 2005. Ocean warming effects on growth, reproduction, and survivorship of southern california abalone. Ecological Applications, 15: 469–480.

Waldbusser, G. G., Voigt, E. P., Bergschneider, H., Green, M. A., and Newell, R. I. E. 2011. Biocalcification in the eastern oyster (*Crassostrea virginica*) in relation to long-term trends in Chesapeake Bay pH. Estuaries and Coasts, 34: 221–231.

Weiss, I. M., Lüke, F., Eichner, N., Guth, C., and Clausen-Schaumann, H. 2013. On the function of chitin synthase extracellular domains in biomineralization. Journal of Structural Biology, 183: 216–225.

Welladsen, H. M., Southgate, P. C., and Heimann, K. 2010. The effects of exposure to near-future levels of ocean acidification on shell characteristics of *Pinctada fucata* (Bivalvia: Pteriidae). Molluscan Research, 30: 125–130.

Wessel, N., Martin, S., Badou, A., Dubois, P., Huchette, S., Julia, V., Nunes, F., et al. 2018. Effect of CO_2–induced ocean acidification on the early development and shell mineralization of the European abalone *Haliotis tuberculata*. Journal of Experimental Marine Biology and Ecology, 508: 52–63.

Winter, B. 2013. Linear models and linear mixed effects models in R with linguistic applications. arXiv: 1308.5499. http://arxiv.org/pdf/1308.5499.pdf

Wittmann, A. C., and Pörtner, H.-O. 2013. Sensitivities of extant animal taxa to ocean acidification. Nature Climate Change, 3: 995–1001.

Wolf-Gladrow, D. A., Zeebe, R. E., Klaas, C., Körtzinger, A., and Dickson, A. G. 2007. Total alkalinity: the explicit conservative expression and its application to biogeochemical processes. Marine Chemistry, 106: 287–300.

Author Queries

Query: AQ1: We have inserted the running head. Please check and provide correct wording if necessary.
Response: Accept

Query: AQ2: Please check all author names and affiliations. Please check that author surnames have been identified by a pink background. This is to ensure that forenames and surnames have been correctly tagged for online indexing.
Response: Sarah: first name (pink) Di Giglio : last name

Query: AQ3: Please provide department name (if any) for affiliations '1–9'.
Response: Accept

Query: AQ4: Please check whether the sentence 'Due to their use …' is OK as given.
Response: Answered within text

Query: AQ5: Please note that journal style specifies 'Abstract should be a single paragraph of not more than 200 words'. Kindly check and confirm the abstract section as it has <200 words.
Response: Accept

Query: AQ6: Please check whether the section hierarchy is OK as set.
Response: Accept

Query: AQ7: If your manuscript has figures or text from other sources, please ensure you have permission from the copyright holder. For any questions about permissions contact jnls.author.support@oup.com.
Response: Accept

Query: AQ8: Please check that all web addresses cited in the text, footnotes and reference list are up-to-date, and please provide a 'last accessed' date for each URL.
Response: Accept

Query: AQ9: Please check that funding is recorded in a separate funding section if applicable. Use the full official names of any funding bodies, and include any grant numbers.
Response: Accept

Query: AQ10: Please note that the “Authors' contributions” section has been retained as given. Please confirm.
Response: Accept

Query: AQ11: Please update the missing volume number and page numbers for Ref. [Auzoux-Bordenave et al. 2019].
Response: Volume number : Marine Biology 167, 11 (2020) doi:10.1007/s00227-019-3623-0

Query: AQ12: Please provide the missing page numbers for Refs. [Cummings et al. 2011; Fitzer et al. 2015].
Response: Cummings V, Hewitt J, Van Rooyen A, Currie K, Beard S, Thrush S, et al. (2011) Ocean Acidification at High Latitudes: Potential Effects on Functioning of the Antarctic Bivalve Laternula elliptica. PLoS ONE 6(1): e16069. https://doi.org/10.1371/journal.pone.0016069Fitzer SC, Zhu W, Tanner KE,Phoenix VR, Kamenos NA, Cusack M. 2015Ocean acidification alters the materialproperties of Mytilus edulis shells. J. R. Soc.Interface 12: 20141227.http://dx.doi.org/10.1098/rsif.2014.1227

Query: AQ13: Please provide the missing publisher location for Ref. [Dickson et al. 2007].
Response: Dickson, A.G., Sabine, C.L. and Christian, J.R. (Eds.) 2007.Guide to Best Practices for Ocean CO2 Measurements.PICES Special Publication 3, 191 pp.Publisher: North Pacific Marine Science Organization, P.O. Box 6000; Sidney, BC V8L 4B2 Canada

Query: AQ14: Please provide the missing editor names for Ref. [IPCC 2014].
Response: IPCC, 2014: Summary for policymakers. In: Climate Change 2014: Impacts, Adaptation, and Vulnerability.Part A: Global and Sectoral Aspects. Contribution of Working Group II to the Fifth Assessment Report of theIntergovernmental Panel on Climate Change [Field, C.B., V.R. Barros, D.J. Dokken, K.J. Mach, M.D. Mastrandrea,T.E. Bilir, M. Chatterjee, K.L. Ebi, Y.O. Estrada, R.C. Genova, B. Girma, E.S. Kissel, A.N. Levy, S. MacCracken,P.R. Mastrandrea, and L.L. White (eds.)]. Cambridge University Press, Cambridge, United Kingdom and NewYork, NY, USA, pp. 1-32

Query: AQ15: Please provide the date that the webpage was accessed for the Refs. [R Core Team 2015 and Winter 2013].
Response: RCoreTeam:Version 3.6.2 (2019-12-12)WInterB.2013.Linear models and linear mixed effects models in R: Tutorial 11Bodo WinterUniversity of California, Merced, Cognitive and Information SciencesLast updated: 01/19/2013; 08/13/2013; 10/01/13; 24/03/14; 24/04/14; 18/07/14; 11/03/16